

NUMERICAL SIMULATION OF THE FLOW IN A CONDUIT, IN THE PRESENCE OF A CONFINED AIR CUSHION

TRIEU DONG NGUYEN*

*Laboratoire d'Etudes des Transferts en Hydrologie et Environnement (INPG, UJF, CNRS UMR 5564, ORSTOM),
B.P. 53X, 38041 Grenoble Cedex, France*

SUMMARY

A rectangular conduit with a closed end has water flowing in/out at the other end. The water level at the open end has an imposed sinusoidal movement. When this level is higher than the ceiling of the conduit, a certain mass of air is trapped under the ceiling. In a previous article (T.D. Nguyen, *La Houille Blanche*, No. 2, 1990), it was supposed that this air is flowing out freely through the ceiling, so the relative pressure at the water surface is zero, and the water hammer at the dead end of the conduit was calculated when the conduit was thoroughly filled. In this article, it is supposed that the trapped air is compressed isothermally or adiabatically. The set of equations is resolved (water continuity and movement equations, air state equation) by supposing a regime of flow at each section (section submerged or not), a certain value for the air pressure and by using the sweep method to determine the water flow characteristics. The air volume calculated by iteration must converge, and the calculated regimes at each section (submerged or free) must agree with the supposed regimes. The simulation is performed first with a horizontal conduit then with an inclined conduit. As expected, adiabatic compression gives higher pressure than isothermal compression. The simulation shows also that when there is an air cushion, compared with the case when air is flowing out freely, the shock of the water hammer at the closed end of the conduit is significantly reduced. This method is aimed at calculating the flow with entrapped air in the inlet/outlet tunnel of a hydroelectric plant, or in sewer system pipe when a sudden discharge surge (due to turbin opening/closing or to urban storm) changes a previously free-surface flow in a mostly full-pipe flow, but with some air entrapped under the ceiling. Copyright © 1999 John Wiley & Sons, Ltd.

KEY WORDS: free-surface/pressurized flow; entrapped air; water hammer

1. INTRODUCTION

In numerical methods to calculate the flow in hydroelectric tunnels or sewer pipes, when an initial free-surface flow becomes a pressurized flow (or full-conduit flow), some authors have used the Saint-Venant equations, with the assumption that acceleration is constant in pressurized flow from upstream boundary to the surge front [1], to calculate water pressure, or with the technique of the so-called 'Preissmann slot', developed by Cunge and Wegner [2]: when pressurized flow occurs, the free-surface level rises in the slot to a certain level depending on the supposed slot width (Figure 1), the pressure in the pressurized flow is given by the water height in the slot. Since then, this technique is used in sewer systems [3,4], with some difficulties

* Correspondence to: Laboratoire d'Etudes des Transferts en Hydrologie et Environnement (INPG, UJF, CNRS UMR 5564, ORSTOM), B.P. 53X, 38041 Grenoble Cedex, France.

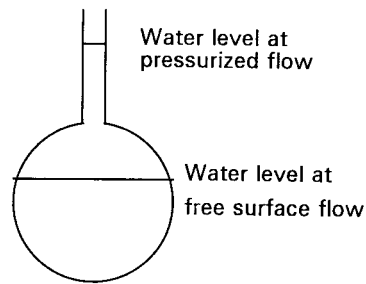


Figure 1. The Preissmann slot.

to determine the water height in the slot [5]. Obviously, this technique supposes that the air over the fluid can flow freely out of the pipe, and there is no entrapped air under the ceiling.

In a previous article [6], the flow in a conduit closed at one end and with water entering at the other end was simulated. At the open end, the water level has an imposed sinusoidal movement (upstream boundary condition), while at the closed end, the downstream boundary condition is $Q = 0$. When the imposed level at entry section is higher than the ceiling, a certain mass of air is trapped under the ceiling. Using water compressibility, water pressure is calculated when it reaches the ceiling, and consequently, the technique of the Preissmann slot is of no use in the current method. With the assumption that trapped air can flow out through the ceiling (so that the relative pressure at the water surface is always zero), the water hammer occurring when the conduit is thoroughly filled was calculated.

In this paper, it is supposed that the ceiling is impervious to air and that the air pocket is progressively compressed when water enters the conduit.

2. HYPOTHESIS

The fluid is submitted to gravity and is compressible, the conduit is supposed rigid. Suppose an elementary length of conduit bounded by a submerged section (SS) and a free section (FS) (the surface line cuts the ceiling line at a point between SS and FS; Figure 2).

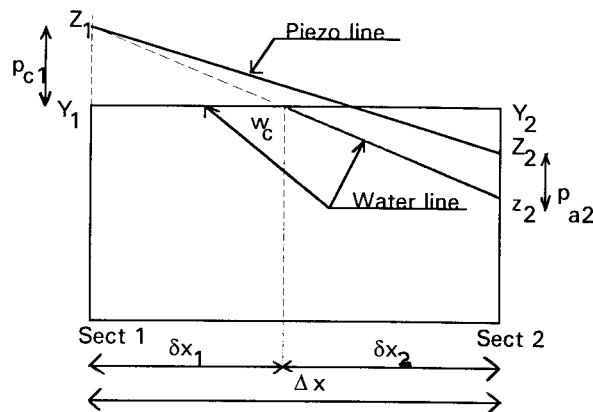


Figure 2. Scheme of an elementary length, with one free section and one submerged.

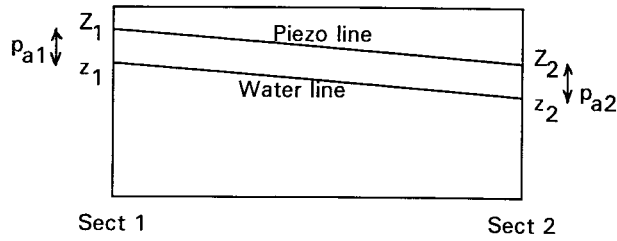


Figure 3. Scheme of an elementary length, with two free sections.

(1) We suppose that the piezometric line is a continuous line through the ceiling, and that the relative pressure of compressed air p_a varies linearly from section 1 to section 2. At section 1 (SS), p_a is zero. The continued water line intersects the piezometric line at Z_1 .

The piezometric height Z is defined by $Z = z + p = z + p_a + p_c$, z being the geometric height, p_c the relative pressure when the fluid is in contact with the ceiling (when the section is submerged). When the fluid is not in contact with the ceiling (at a free section), p_c is zero. The pressures p_a and p_c are evaluated in height of water. In Figure 2, $p_{c1} \neq 0$ and $p_{c2} = 0$. On the contrary, for p_a from the compressed air, $p_{a1} = 0$ and $p_{a2} \neq 0$. To simplify the calculations, suppose a linear variation of Z and air pressure p_a in Δx . Strickly speaking, where the fluid comes in contact with the ceiling (from section 1 to point w_c), there is no more air and consequently $p_a = 0$.

(2) When the two boundary sections are free (Figure 3), p_a is constant in Δx ($p_{a1} = p_{a2}$). The piezometric line and water line are parallel.

(3) The compression of the trapped air is sufficiently rapid, so there is no dissolving of air in water (the mass of trapped air is constant).

3. CONSIDERED SET OF EQUATIONS

The system of equations is composed of two equations of continuity and movement for compressible water when there is a linearly variable pressure at its surface, and one state equation for air.

3.1. Equations of continuity and movement for water

3.1.1. Equation of continuity. The liquid volume between sections 1 and 2 is (Figure 2):

$$V_1 = \frac{\Delta x}{2} \left\{ S_1 + S_2 - \frac{\delta x_1}{\Delta x} (S_1 - AM_1) - \frac{\delta x_2}{\Delta x} (S_2 - AM_2) \right\}.$$

The air volume is:

$$V_a = \frac{\Delta x}{2} \left\{ \frac{\delta x_1}{\Delta x} (S_1 - AM_1) + \frac{\delta x_2}{\Delta x} (S_2 - AM_2) \right\}.$$

Of course, we have:

$$V_1 + V_a = \frac{\Delta x}{2} (S_1 + S_2) = \text{inside volume of an elementary length of conduit.}$$

The lengths δx_1 and δx_2 are defined by:

$$\frac{\delta x_1}{\Delta x} = \frac{(Z_1 - p_{a1}) - Y_1}{Y_2 - Y_1 - \{(Z_2 - p_{a2}) - (Z_1 - p_{a1})\}},$$

$$\frac{\delta x_2}{\Delta x} = 1 - \frac{\delta x_1}{\Delta x}.$$

The equation of continuity is written as:

$$\frac{\partial Q}{\partial x} + \frac{\partial A}{\partial t} + \frac{A}{\rho} \frac{\partial \rho}{\partial t} = 0.$$

As the wetted area A is defined from the liquid volume V_1 in an elementary length Δx by $A = V_1/\Delta x$,

$$\frac{\partial A}{\partial t} = \frac{1}{2} \left(b_{1e} \frac{\partial(Z_1 - p_{a1})}{\partial t} + b_{2e} \frac{\partial(Z_2 - p_{a2})}{\partial t} \right),$$

and the specific mass variation is equal to:

$$\frac{\partial \rho}{\partial t} = \frac{1}{2} \rho_0 \sigma_0 \beta \left\{ \frac{\partial(p_{c1} + p_{a1})}{\partial t} + \frac{\partial(p_{c2} + p_{a2})}{\partial t} \right\}.$$

The equivalent widths b_{1e} and b_{2e} , equal to the conduit widths at free sections, are given in Appendix A.

3.1.2. Equation of movement.

$$gA \frac{\partial Z}{\partial x} + gAS_f + \frac{\partial Q}{\partial t} + U \frac{\partial Q}{\partial x} - U \left(\frac{\partial A}{\partial t} + U \frac{\partial A}{\partial x} \right) = 0.$$

The first part is coming from the projected pressure force on the upper face, the pressure forces on the upstream and downstream faces and from the projected weight, the second part from the friction force and the third part from the inertial force (see Appendix B; Figure 4). When there is no contact with the ceiling ($p_c = 0$) and the air pressure is zero ($p_a = 0$), you have $Z = z$, and if the fluid is also incompressible ($\partial \rho / \partial t = 0$), the two above equations are the Saint-Venant equations.

3.2. State equation for air

For an isolated mass of air of volume V_a , subject to absolute pressure P_a , the relation: $P_a V_a^\gamma = Cste$.

With differential form, and with $P_a = p_a + 10$, the absolute and relative pressures P_a and p_a are both evaluated in water height:

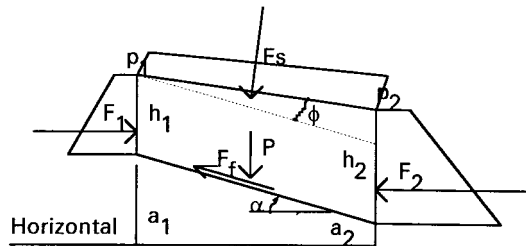


Figure 4. Forces on an elementary water body, with variable pressure on the water surface.

$$\frac{dp_a}{dt} + \frac{P_a \gamma}{V_a} \times \frac{dV_a}{dt} = 0.$$

For an elementary length Δx , $dV_a = -dV_1 = -\Delta x \cdot dA$. So, if air mass occupies the upper part of N elementary lengths limited by sections i and $i + 1$, the variation of air volume is given by:

$$\frac{dV_a}{dt} = \frac{1}{2} \sum_{i=1}^N \Delta x_i \left(-b_{1ei} \frac{\partial Z_i}{\partial t} - b_{2ei} \frac{\partial Z_{i+1}}{\partial t} + (b_{1ei} + b_{2ei}) \frac{dp_a}{dt} \right).$$

From which we have the differential form of state equation of the trapped air:

$$\frac{dp_a}{dt} \left\{ 1 + \frac{P_a \gamma}{V_a} \frac{1}{2} \sum_{i=1}^N \Delta x_i (b_{1ei} + b_{2ei}) \right\} = \frac{P_a \gamma}{V_a} \frac{1}{2} \sum_{i=1}^N \Delta x_i \left(b_{1ei} \frac{\partial Z_i}{\partial t} + b_{2ei} \frac{\partial Z_{i+1}}{\partial t} \right).$$

4. METHOD OF RESOLUTION

Suppose a known state of flow at time t : at each section, the regime (submerged or free) is known, as is the piezometric height Z , the discharge Q and the air pressure p_a , and these variables must be determined at time $t = t + \Delta t$. Except for the first section in the application below, a boundary section, and where the regime is determined by boundary level condition, we suppose first that the regime at each section is the same as at time t . By a double sweep method and using boundary conditions, ΔZ and ΔQ are determined with the two continuity and movement equations for water. For each reach Δx and each time increment Δt , the two equations are discretized by finite difference method, with the implicit Preismann scheme [6]. The space weighting coefficient is equal to 0.5 and the time weighting coefficient is taken equal to 0.87. Then the calculated ΔZ are used in the state equation for air to determine Δp_a , consequently, a new value for p_a to be injected in the two equations for water is obtained. Proceeding by iterations, a set of values for ΔZ , ΔQ and Δp_a is obtained, satisfying the three differential equations. At each iteration, that the regime (submerged or not) at each section remains the same must be verified, i.e. a submerged/free section remains submerged/free. Otherwise, if a free section becomes submerged, or vice versa, we must introduce in these equations the known quantities Δz_i , Δp_{ai} or Δp_{ci} . For example, a previously free section i becomes submerged: we write that the water is in contact with the ceiling ($\Delta z_i = Y_i - z_i^n$) and the air pressure becomes zero ($\Delta p_{ai} = 0 - p_{ai}^n$); we must now calculate $\Delta p_{ci} = p_{ci}^{n+1} - 0$ and verify that the water is compressed by the ceiling with $\Delta p_{ci} > 0$. In the inverse way, when a previously submerged section i becomes free, it is known that the variation of pressure due to ceiling $\Delta p_{ci} = 0 - p_{ci}^n$. The air pressure on the newly free section is equal to the pocket air pressure (equal air pressure on free sections is admitted, see Figure 3), so $\Delta p_{ai} = p_a^{n+1} - 0$. Now, calculate $\Delta z_i = z_i^{n+1} - Y_i$ and the new air pressure p_a^{n+1} by iterations and verify that the free-surface is under the ceiling, i.e. $\Delta z_i < 0$.

5. APPLICATION

A rectangular conduit of section $76.2 \text{ m} \times 61000 \text{ m}$, of length 305000 m , with a closed end and with water flowing in/out at the other end is studied. The length and width of the conduit are those of a parallelepipedic estuary in which Wen Hsiung Li [7] had treated the movement of a body of water bounded laterally and at one end by walls and submitted to periodical surface

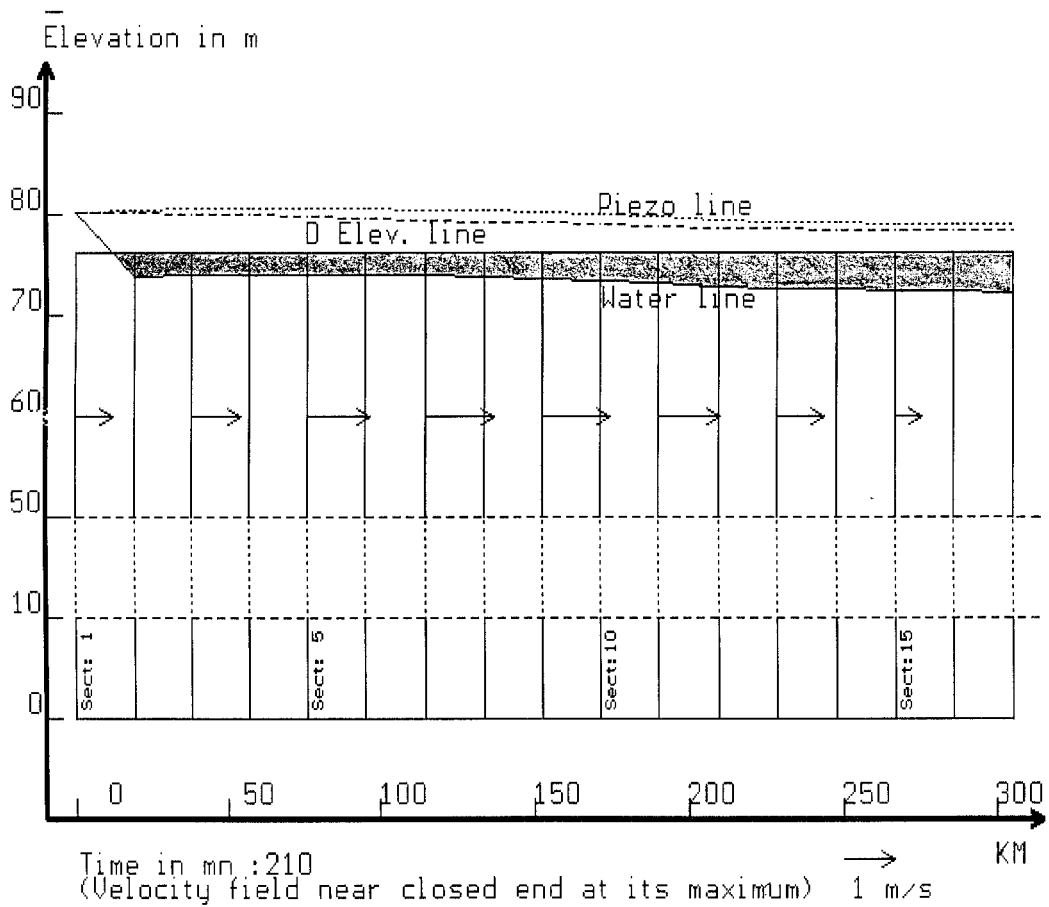


Figure 5. Isothermal compression. Piezometric, water, D elevation lines and velocity field.

tide movement at the other end (the tide has an amplitude of 4.42 m and a period of $T = 12.4$ h). In the present model, a ceiling has been put at the tide mean level, so when the level at the entry end is higher than the ceiling, a certain mass of air is trapped under the ceiling. The conduit is divided in 16 equal reaches by 17 transects. First it is placed horizontally ($da/dx = 0$), then slightly upwards at the closed end ($da/dx = 10^{-5}$). Previously, flow in the model was verified when all sections are free (when the water surface is under the ceiling) with the analytical formulae given by Wen Hsiung Li [7]. Then when the boundary level at the entry section is higher than the ceiling, it was supposed that the trapped air can flow freely out through the ceiling (so $p_a = 0$), the water hammer occurring when the conduit is entirely filled was calculated [6]. In the present paper, it is supposed that the ceiling is impervious to air and that the trapped air is compressed isothermally ($\gamma = 1$), or adiabatically ($\gamma = 1.4$) and that the air pressure is the same at free sections ($\partial p_a / \partial x = 0$).

When the conduit is horizontal (Figure 5), the piezometric line and water line occur when incoming velocities near the closed end are at their maximum, in case of isothermal compression. Figures 6 and 7 show piezometric and water lines at the moment of minimum air volume (Figure 6 for isothermal compression and Figure 7 for adiabatic compression). It is noticed that for isothermal compression (Figure 6), three sections at the dead end are submerged at

this instant. Figure 8 presents the variation with time of air pressure and air volume. Notice that for a same trapped air mass, adiabatic compression gives higher pressure and consequently higher volume than isothermal compression. Figures 9 and 10 present variations of water velocity with time for some sections near the dead end (Figure 9 for isothermal compression and Figure 10 for adiabatic compression). In isothermal compression (Figure 9), the sudden surge of velocity at time about 300 min is due to sudden change in water surface slope, when previously free sections near the dead end become submerged (see Figure 6: instead of the supposed straight line between FS and SS, a more natural curved link between FS and SS—represented by dashed line in Figure 6—will diminish the volume offered to water and consequently will dampen this velocity surge). This phenomenon does not appear in adiabatic compression, where near dead end sections remain free during compression.

Having no possibility of comparing the present results with analogous works, an ‘internal’ verification is performed as follows: from the above calculated velocity field $U(x, t)$, we use the generalized Bernoulli equation inferred from the movement equation:

$$D(x, t) = Z(x, t) + \frac{1}{2g} [U(x, t)]^2 + \frac{1}{g} \int_0^x \frac{\partial U}{\partial t} dx = Z(0, t) + \frac{1}{2g} [U(0, t)]^2 - \int_0^x S_f dx,$$

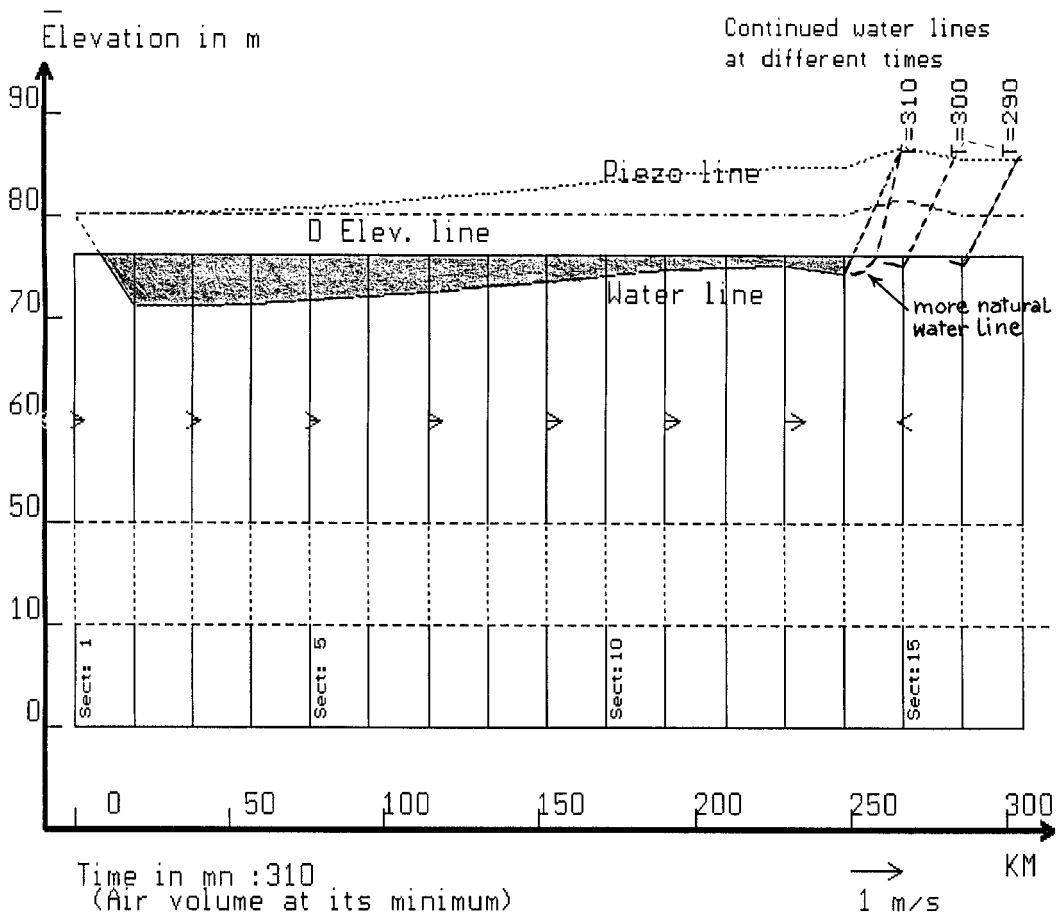


Figure 6. Isothermal compression. Piezometric, water, D elevation lines at minimum air volume.

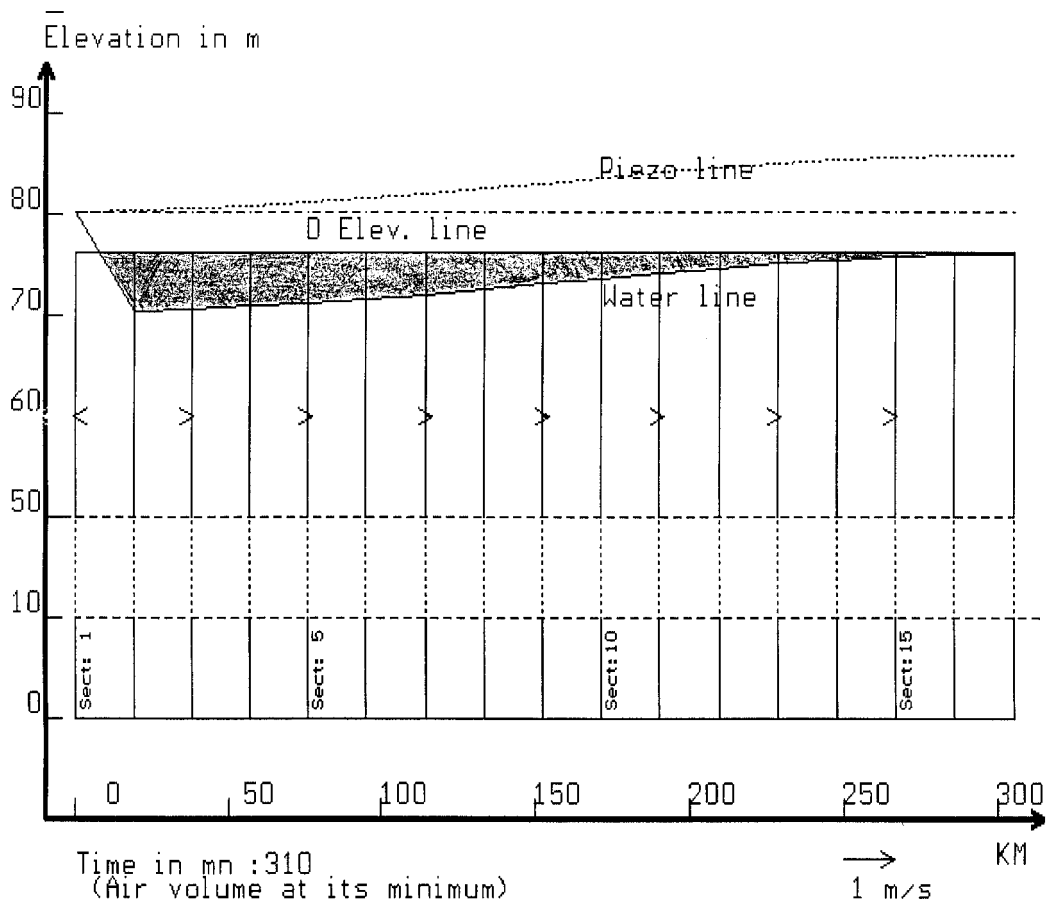


Figure 7. Adiabatic compression. Piezometric, water, D elevation lines at minimum air volume.

to recalculate Z from this integral equation. The Z determined with the present method and that calculated from the Bernoulli equation are almost the same. For example, in the case of isothermal compression (Figure 6), in the following table some numerical values at different sections are given:

Section	1 (Boundary)	5	10	15	17
Z (m) this paper	80.200	80.818	83.376	86.813	85.580
Z (m) Bernoulli	80.200	80.657	83.118	85.024	85.625

It is also remarked that the D elevation defined above has an usual falling slope S_f in direction of flow. This elevation is also given in figures, along with piezometric and water lines. When the air volume is at its minimum (Figures 6, 7 and 11), this line is quasi-horizontal, due to small velocity and small value for S_f . In Figure 6, the error of small uprise of the D elevation line at section 15 is the consequence of error of surge of velocity (Figure 9), as the link between FS and SS must be modeled by a straight line.

In the following table, at the closed end section (section 17), maximum values of p_c (when section is submerged) or p_a (when it is free) are given, in case of air flowing out freely (no air pocket) and in case of air compressed isothermally or adiabatically (with air pocket). When there is an air cushion there is no more surge in pressure at this wall (no water hammer effect), and the pressure at this end is reduced significantly.

Closed end section regime at maximum pressure	Submerged section (air flowing out freely)	Submerged section (air compressed isothermally)	Free section (air compressed adiabatically)
Pressure in metres of water	48	10.4	10.1

When the conduit is inclined, for isothermal compression, Figure 11 shows the piezometric, water and D elevation lines at the moment of minimum air volume. Notice that compared with compression in horizontal conduit, more sections at the entry end become submerged (two

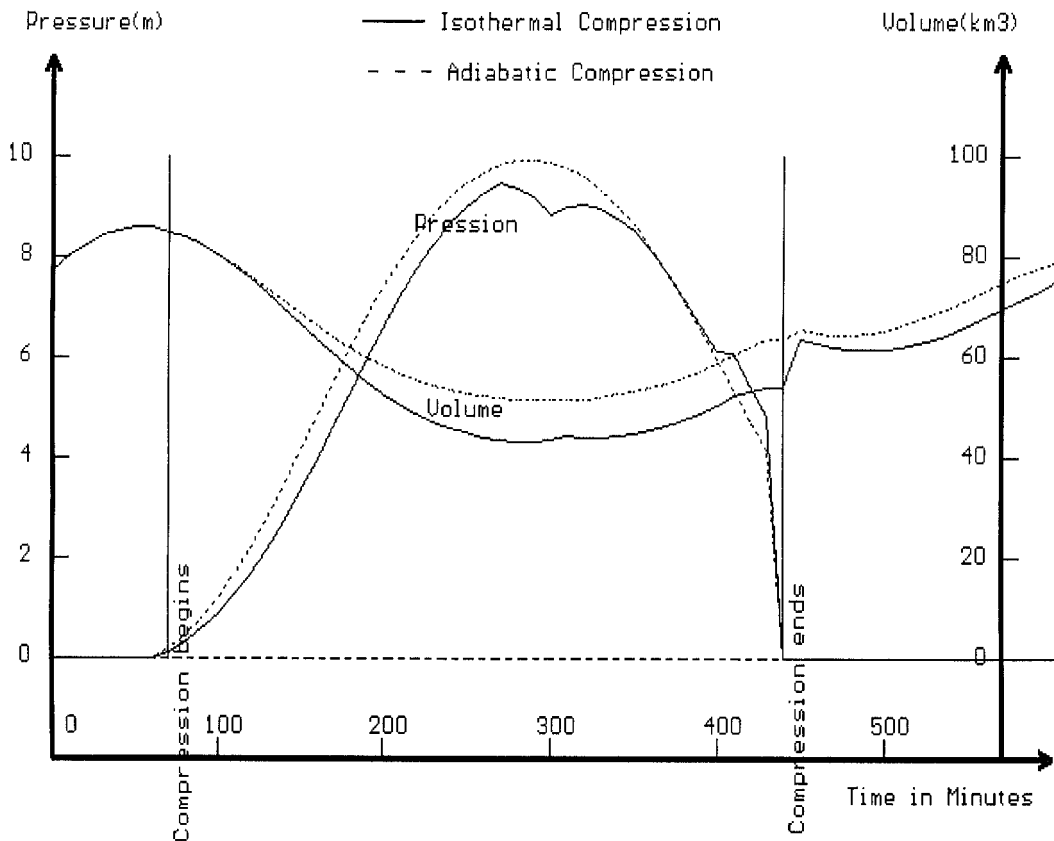


Figure 8. Variation with time of air pressure and volume.

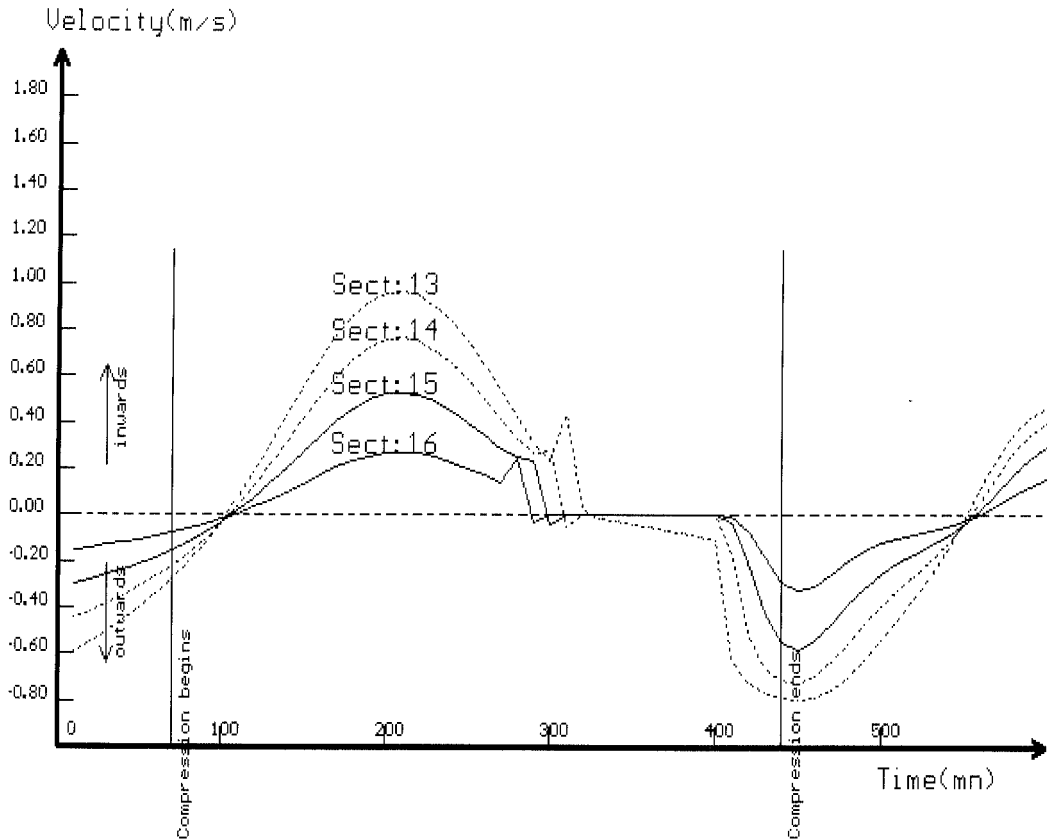


Figure 9. Isothermal compression. Variation of velocities with time.

sections submerged instead of 1 submerged section with horizontal conduit) and there are no more submerged sections at dead end.

6. CONCLUSION

In this article, the problem of water flow inside a closed conduit, in the presence of a trapped air cushion, is treated by numerical simulation. This kind of flow may occur in sewer pipes or hydroelectric tunnels. The considered application deals with a conduit of very large dimensions, in fact the dimensions of an estuary, for the sake of comparison, when flow is a free-surface flow, between this paper's results and Wen Hsiung Li analytical results [7]. But one of the advantages of numerical methods is to change easily geometric and dynamic input: so in case of no air pocket, the transition from free-surface flow to pressurized flow in an hydroelectric pressure pipe had already been simulated (steel pipe of diameter 1500 mm, of thickness 55 mm), with simulation of the water hammer intensity, when the gate at the end of the pipe is progressively shut (see [6]). In the current simulation, when an air pocket is present, the next stage of study is to find a concrete case of application, with measures of air pressure and water flow characteristics, for comparison between numerical simulation results and experimental or on site measures.

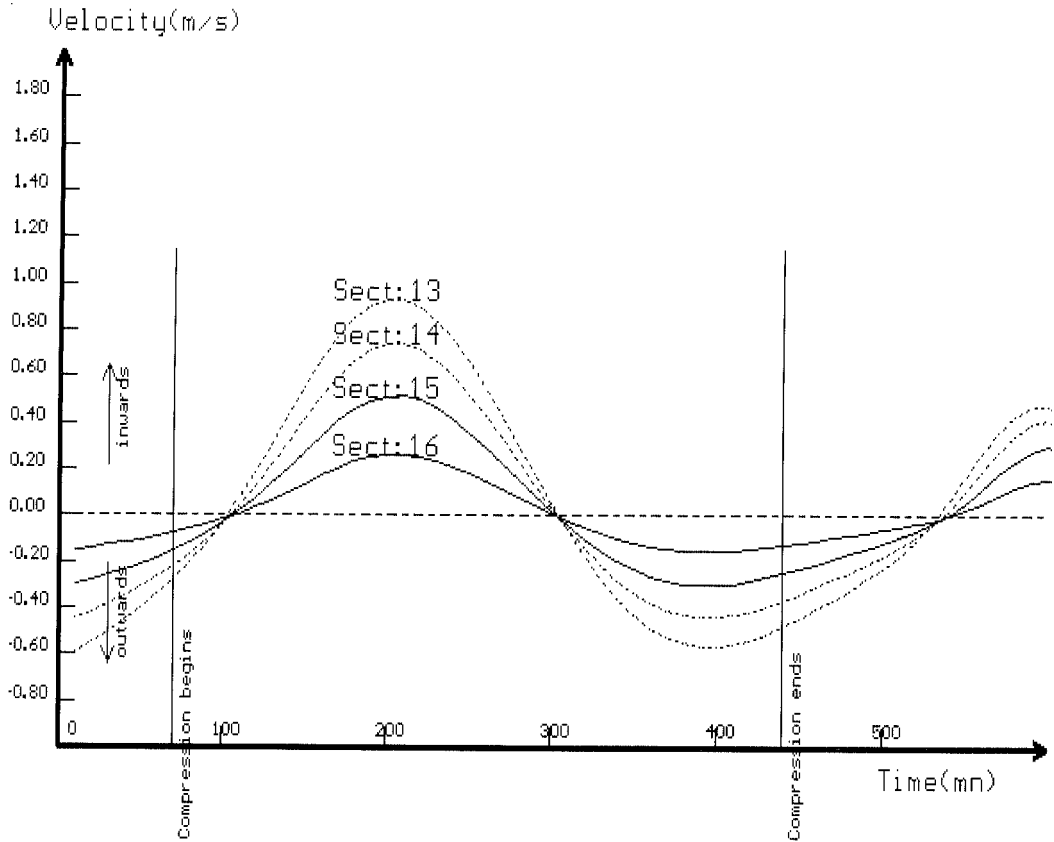


Figure 10. Adiabatic compression. Variation of velocities with time.

APPENDIX A

The equivalent widths b_{1e} and b_{2e} are given by:

(a) When the water line cuts the ceiling line in the elementary length Δx (Figure 2),

$$b_{1e} = b_1 \cdot \frac{\delta x_1}{\Delta x} - \frac{S_1 - AM_1 - (S_2 - AM_2)}{Y_2 - Y_1 - (Z_2 - p_{a2} - (Z_1 - p_{a1}))} \cdot \frac{\delta x_2}{\Delta x},$$

$$b_{2e} = b_2 \cdot \frac{\delta x_2}{\Delta x} - \frac{S_1 - AM_1 - (S_2 - AM_2)}{Y_2 - Y_1 - (Z_2 - p_{a2} - (Z_1 - p_{a1}))} \cdot \frac{\delta x_2}{\Delta x}.$$

In the case of Figure 2, where section 1 is submerged, $p_{a1} = 0$.

(b) When the water line is entirely under the ceiling line (Figure 3),

$$b_{1e} = b_1,$$

$$b_{2e} = b_2.$$

(c) When the water line coincides with the ceiling line, and as the conduit is supposed rigid,

$$b_{1e} = 0, \quad b_{2e} = 0.$$

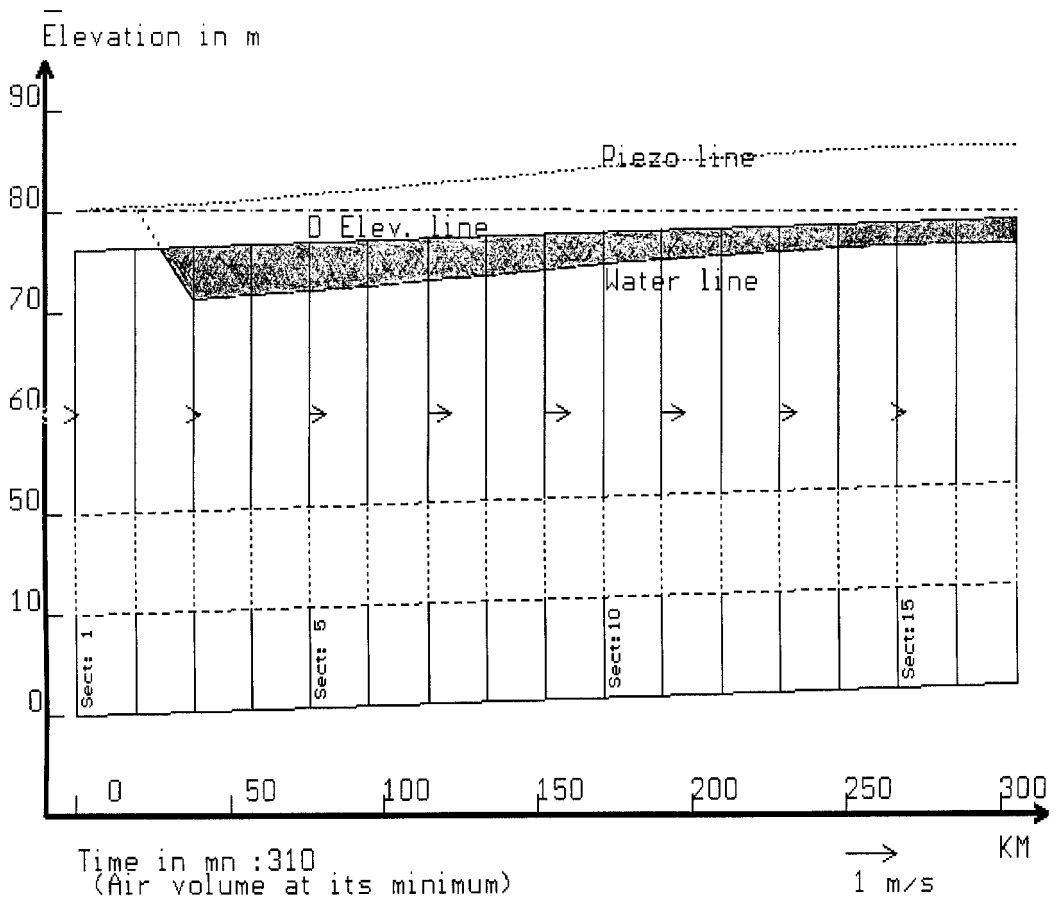


Figure 11. Inclined conduit. Isothermal compression. Piezometric, water lines at minimum air volume.

APPENDIX B

(See Figure 4.)

For a Δx length of a water body in a rectangular channel of unit width, submitted to weight P , bottom friction force and pressure forces F_1 and F_2 on upstream and downstream sections and F_s on the water surface, let:

$$Z_1 = a_1 + h_1 + p_1; \quad Z_2 = a_2 + h_2 + p_2.$$

We have:

$$\frac{F_1}{\omega_0} = p_1 h_1 + \frac{h_1^2}{2} = \frac{1}{2} (h_1 + p_1)^2 - \frac{p_1^2}{2} = \frac{1}{2} (Z_1 - a_1)^2 - \frac{p_1^2}{2},$$

$$\frac{F_2}{\omega_0} = \frac{1}{2} (Z_2 - a_2)^2 - \frac{p_2^2}{2},$$

$$\frac{F_s}{\omega_0} = \frac{p_1 + p_2}{2} \Delta x.$$

Now:

$$\begin{aligned}\frac{F_1 - F_2}{\varpi_0} &= \frac{1}{2} [(Z_1 - a_1)^2 - (Z_2 - a_2)^2] + \frac{1}{2} (p_2^2 - p_1^2) \\ &= \left(-\frac{\partial Z}{\partial x} \Delta x + \frac{\partial a}{\partial x} \Delta x \right) (Z_m - a_m) + \frac{\partial p}{\partial x} \Delta x \cdot p_m.\end{aligned}$$

But:

$$\frac{\partial a}{\partial x} \Delta x (Z_m - a_m) = \frac{\partial a}{\partial x} \Delta x (Z_m - a_m - p_m + p_m) = \frac{\partial a}{\partial x} \Delta x (h_m + p_m) \cong -\frac{P}{\varpi_0} \sin \alpha + p_m \frac{\partial a}{\partial x} \Delta x.$$

So:

$$\frac{P \sin \alpha + F_1 - F_2}{\varpi_0} = -\Delta x (Z_m - a_m) \frac{\partial Z}{\partial x} + \Delta x \cdot p_m \left(\frac{\partial p}{\partial x} + \frac{\partial a}{\partial x} \right).$$

The projection of F_s on the bottom line is equal to:

$$\frac{F_s}{\varpi_0} \cdot \sin(\phi) = p_m \cdot \Delta x \cdot \frac{\partial h}{\partial x}.$$

Finally,

$$\frac{P \sin \alpha + F_1 - F_2 + F_s \sin \phi}{\varpi_0} = -\Delta x \cdot h_m \cdot \frac{\partial Z}{\partial x}$$

and for a channel of mean width b_m

$$P \sin \alpha + F_1 - F_2 + F_s \sin \phi = -\varpi_0 \cdot \Delta x \cdot b_m \cdot h_m \cdot \frac{\partial Z}{\partial x} = -\varpi_0 \cdot \Delta x \cdot A_m \cdot \frac{\partial Z}{\partial x}.$$

Part 2: the friction force is equal to: $-S_f \varpi_0 A_m \Delta x$.

Part 3: the inertial force is equal to $-\rho A_m \Delta x \Gamma$, with acceleration Γ equal to:

$$\Gamma = \frac{1}{A_m} \left\{ \frac{\partial Q_m}{\partial t} + U_m \frac{\partial Q_m}{\partial x} - U_m \left(\frac{\partial A_m}{\partial t} + U_m \frac{\partial A_m}{\partial x} \right) \right\}.$$

APPENDIX C. NOMENCLATURE

a	bottom elevation (m)
A	wetted area defined from the liquid volume V_1 by $A = V_1/\Delta x$ (m ²)
AM	wetted area at a conduit section (m ²)
A_m :	mean wetted area for two consecutive transsects (m ²) ($A_m = 0.5 \times (AM_1 + AM_2)$)
b	width at the free surface (m)
b_{1e}, b_{2e}	equivalent widths, given in Appendix A (m)
D	elevation, defined as $D(x, t) = Z(x, t) + 1/2g [U(x, t)]^2 + 1/g \int_0^x \partial U/\partial t \, dx$ (m)
g	gravity acceleration (m s ⁻²)
K	Strickler coefficient (m ^{1/3} s ⁻¹)
p	pressure on water surface, evaluated in water height (m); $p = p_a$ at a free section and $p = p_c$ at a submerged section
P_a	absolute pressure of trapped air (m)

Q	discharge ($\text{m}^3 \text{s}^{-1}$)
S	area of a section of the conduit (m^2)
S_f	friction slope ($S_f = Q_m Q_m / K^2 A_m^2 (R/h_m)^{4/3}$)
t	time (s)
T	oscillating level period at the open end of the example conduit ($T = 12.4 \times 3600$ s)
U	velocity (m s^{-1}) ($U = Q/AM$)
V_1	liquid volume in an elementary length (m^3)
V_a	air volume in an elementary length (m^3)
x	longitudinal abscissa, directed positively from open end to closed end of conduit (m)
Y	ceiling elevation (m)
z	water surface elevation (m)
Z	piezometric elevation, defined as $Z = z + p = z + p_a + p_c$ (m)
α	bottom slope
β	water compressibility ratio ($\beta = 5 \times 10^{-10} \text{ m}^2 \text{ N}^{-1}$)
γ	constant in air state equation
ϕ	angle between water line and bottom line
ρ_0	water specific mass at $p = 0$ (kg m^{-3})
ϖ_0	water specific weight at $p = 0$ (9810 N m^{-3})
Γ	water acceleration (m s^{-2})
$\Delta f_i = f_i^{n+1} - f_i^n$	

Suffix m marks the mean value for two consecutive transsects (e.g. $b_m = 0.5 \times (b_1 + b_2)$)

Suffix 1, 2 mark the serial number of transsects (e.g. F_1 : pressure force on transsect 1)

Power index n marks time step ($t = n\Delta t$)

FS, free section; SS, submerged section.

REFERENCES

1. D.C. Wiggert, 'Transient flow in free surface, pressurized systems', *J. Hydraul. Div., ASCE*, HY1, **98**, 11 (1972).
2. J.A. Cunge and M. Wegner, 'Intégration numérique des équations d'écoulement de Barré de Saint-Venant par un schéma implicite de différences finies. Application au cas d'une galerie tantôt en charge tantôt à surface libre', *La Houille Blanche*, No. 1, 1964, p. 33 (in French).
3. F.M. Holly Jr., G. Chevereau and B. Mazaudou, 'Numerical simulation of unsteady flow in storm sewer systems using complete and simplified flow equations', *Int. Conf. on Numerical Modelling*, Bratislava, Czechoslovakia, 1981.
4. J.E. Ball, 'An algorithm for routing unsteady flows in urban drainage networks', *J. Hydraul. Res.*, **23**, 327 (1985).
5. J.A. Cunge and B. Mazaudou, 'Mathematical modelling of complex surcharge systems: difficulties in computation and simulation of physical situations', *Int. Conf. on Urban Storm Drainage*, Göteborg, Sweden, 1984, p. 363.
6. Trieu Dong Nguyen, 'Sur une méthode numérique de calcul des écoulements non permanents soit à surface libre, soit en charge, soit partiellement à surface libre et partiellement en charge', *La Houille Blanche*, No. 2, 1990, p. 149 (in French).
7. Wen Hsiung Li, 'Well mixed estuaries with non linear resistance', *J. Hydraul. Res.*, **12**, 83 (1974).